CRISPRi is not strand-specific and redefines the transcriptional landscape

Françoise S. Howe[1], Andrew Russell[1], Afaf El-Sagheer[2,3], Anitha Nair[1], Tom Brown[2] and Jane Mellor[1]*.

[1] Department of Biochemistry, University of Oxford, South Parks Road, Oxford, OX1 3QU, UK

[2]Department of Chemistry, Chemistry Research Laboratory, University of Oxford, South Parks Road, Oxford, OX1 3TA, UK

[3]Chemistry Branch, Faculty of Petroleum and Mining Engineering, Suez University, Suez 43721, Egypt.

* Correspondence: jane.mellor@bioch.ox.ac.uk

ABSTRACT

CRISPRi, an adapted CRISPR-Cas9 system, is proposed to act as a strand-specific roadblock to repress transcription in eukaryotic cells using guide RNAs (sgRNAs) to target catalytically inactive Cas9 (dCas9) and offers an alternative to genetic interventions for studying pervasive antisense transcription. Here we successfully use click chemistry to construct DNA templates for sgRNA expression and show, rather than acting simply as a roadblock, binding of sgRNA/dCas9 creates an environment that is permissive for transcription initiation and termination, thus generating novel sense and antisense transcripts. At *HMS2* in *Saccharomyces cerevisiae*, sgRNA/dCas9 targeting to the non-template strand results in antisense transcription termination, premature termination of a proportion of sense transcripts and initiation of a novel antisense transcript downstream of the sgRNA/dCas9 binding site. This redefinition of the transcriptional landscape by CRISPRi demonstrates that it is not strand-specific and highlights the controls and locus understanding required to properly interpret results from CRISPRi interventions.

INTRODUCTION

Eukaryotic genomes are pervasively transcribed but the effect of this inter- and intragenic transcription is not fully understood (Mellor, Woloszczuk, & Howe, 2016). Of particular interest is the function of antisense transcription, which alters the chromatin in the vicinity of sense promoters (Lavender et al., 2016; Murray et al., 2015; Pelechano & Steinmetz, 2013), and is associated with repression, activation or no change in levels of the corresponding sense transcript (Murray et al., 2015). Discerning the mechanism by which antisense transcription functions in gene regulation is confounded by the difficulty in ablating antisense transcription without direct genetic intervention (Bassett et al., 2014). A new approach, CRISPR interference (CRISPRi) (Qi et al. 2013), can circumvent these issues by avoiding the need to manipulate endogenous DNA sequences. An endonucleolytically dead version of Cas9 (dCas9) is recruited by single base pairing guide RNAs (sgRNAs) targeting the non-template (NT) DNA strand, where it blocks transcription strand-specifically at the loci tested (Lenstra, Coulon, Chow, & Larson, 2015; Qi et al., 2013). In a further adaptation, dCas9 fusion with transcriptional repressors or activators allows both negative and positive regulation of transcription respectively (Gilbert et al., 2013, 2014), but the strand-specificity is lost and thus is not suitable for strand-specific repression of antisense transcription. The sgRNA compenent of the CRISPRi system consists of two regions: a constant region (82 nt) that binds to dCas9 and a variable region (20 nt) that is responsible for targeting. The modular nature of the sgRNA lends itself to synthetic copper(I)-catalysed alkyne-azide cycloaddition (CuAAC) click chemistry (El-Sagheer & Brown, 2010). The stable artificial triazole DNA linker generated is biocompatibile, being read and accurately copied by DNA and RNA polymerases (Birts et al., 2014; El-Sagheer & Brown, 2011; El-Sagheer, Sanzone, Gao, Tavassoli, & Brown, 2011). We show that click chemistry is an efficient method for sgRNA construction and that when combined with dCas9, these sgRNAs are as effective as sgRNAs produced from chemically synthesised full-length DNA templates at reducing levels of transcripts *in vivo*. However, it is still not completely understood how the CRISPRi system functions strand-specifically or why sgRNAs must target the non-template strand.

Here we use the CRISPRi system to study the effect of blocking antisense transcription at loci with well characterised sense:antisense transcript pairs. We have previously used a promoter deletion of the antisense transcript *SUT650* at the *HMS2* locus to show that *SUT650* represses *HMS2* sense transcription (Nguyen et al., 2014). Now we use CRISPRi to examine the effects of blocking *SUT650* antisense transcription to ask (i) whether *SUT650* represses *HMS2* sense transcription *without* a genetic intervention and (ii) whether CRISPRi is strand-specific using, in addition to *HMS2*, an engineered *GAL1* gene with a well characterised antisense transcript (Murray et al., 2012, 2015).

The main conclusion from this study is that CRISPRi at the *HMS2* locus is not fully strand-specific and results in (i) premature termination of the sense transcript and (ii) initiation of a new unstable antisense transcript in the vicinity of the sgRNA binding site. As transcription from this new antisense initiation site extends in to the *HMS2* promoter, there is no net change in *HMS2* sense transcript levels. Thus CRISPRi redefines the transcriptional landscape at *HMS2*. This suggests that routine use of CRISPRi for gene expression analysis will require rigorous analysis of transcript integrity and function before conclusions can be drawn.

RESULTS & DISCUSSION

DNA templates for sgRNA production can be made using click chemistry

CRISPRi-mediated transcriptional repression requires co-expression of a mature sgRNA and dCas9 (Fig 1A). A small library of single-stranded DNAs, comprised of templates for sgRNA variable regions, were joined to the constant region using click chemistry (Fig. 1B) and used successfully as templates for PCR, with no significantly different efficiencies when compared to control full-length synthesised oligonucleotides (Fig. 1C). The PCR products were inserted in place of a *URA3* selection cassette in the endogenous *snR52* locus for expression of a transcript that is then processed to form the mature nuclear-retained sgRNA (Fig. 1A). Levels of dCas9 protein were uniform between strains (Fig. 1 – Figure Supplement 1). Neither insertion of *URA3* into snR52 nor dCas9 expression in the control

strains affected growth rate, although strains expressing some sgRNAs grew more slowly indicating a physiological effect (Fig. 1D).

CRISPRi represses the production of antisense transcripts at *HMS2* and *GAL1*

CRISPRi represses transcription when sgRNAs/dCas9 are targeted to the non-template (NT) strand next to a protospacer adjacent motif (PAM) (Qi et al., 2013) (Fig. 2A). Firstly, we used an engineered version of *GAL1* that has a stable antisense transcript (*GAL1* AS) initiating within an *ADH1* terminator inserted into the *GAL1* coding region (Murray et al., 2012) (Fig. 2B). *GAL1* AS is present in cells grown in glucose-containing media when the *GAL1* gene is repressed and is reduced as cells are switched into galactose-containing media and *GAL1* sense is induced (Fig. 2C lanes 1-3). We designed sgRNAs adjacent to two PAM sequences on the non-template strand near the antisense transcription start site (TSS) (AS+28NT and AS+112NT) and a third strand-specificity control sgRNA on the template strand in this region (AS+93T) (Fig. 2B). Only sgRNA AS+112NT/dCas9 caused significant (p=0.016) reduction in *GAL1* antisense transcript levels, as assessed by Northern blotting (Fig. 2C,D).

Next, we examined the *HMS2* locus which has a stable antisense transcript, *SUT650*, initiating within the 3' coding region of *HMS2* (Nguyen et al., 2014; Pelechano, Wei, & Steinmetz, 2013). We designed three *SUT650*-targeting sgRNAs, one acting as a control located 44 nucleotides upstream of the *SUT650* TSS on the non-template strand (AS-44NT), and two sgRNAs, AS+148NT and AS+181NT, targeting sequences downstream of the TSS (Fig. 2E). AS+148NT/dCas9 significantly (p=0.011) reduced *SUT650* (Fig. 2F lanes 1&3, 2G) and this repression was comparable for the clicked and control full-length synthetic constructs (Fig. 2G). However, there was no obvious effect of the other two sgRNAs/dCas9 on *SUT650* levels (Fig. 2F lanes 1, 4&5, 2G). CRISPR efficiency has been linked to nucleosome occupancy (Horlbeck, Witkowsky, et al., 2016; Isaac et al., 2016) but we found no correlation between the level of repression and the nucleosome occupancy (Knight et al., 2014) at each of the *SUT650* sgRNA target regions (Fig. 2 – Figure Supplement 1). However, other factors such as sequence determinants can also influence repression (Horlbeck, Gilbert, & Villalta, 2016). These

results at *GAL1* and *HMS2* confirm CRISPRi is suitable for reducing levels of antisense transcripts in yeast but controls are needed for each sgRNA designed to ensure that repression has been achieved.

CRISPRi repression of *SUT650* induces a new shorter antisense transcript at *HMS2*

At *HMS2*, sgRNA AS+148NT/dCas9 was able to reduce *SUT650* levels significantly (Fig. 2F,G). Since *SUT650* is a substrate for the major cytoplasmic 5'-3' exonuclease Xrn1 (Fig. 2F, lanes 1&2), we investigated whether the CRISPRi-induced *SUT650* reduction was due to direct repression of antisense transcription and/or a reduction in *SUT650* stability. Whilst *SUT650* was not stabilised upon *XRN1* deletion in the strain expressing AS+148NT/dCas9, supporting previous studies that CRISPRi operates via a transcriptional block (Qi et al., 2013) (Fig. 2F, lanes 3&6, transcript B), we detected a shorter antisense transcript (Fig 2F, lane 6, transcript B^t). To map transcript B^t, we used a series of Northern blotting probes across the locus (Fig. 2H). With antisense-specific probes H1 and H2 in the *HMS2* gene promoter and 5' coding region respectively, we could detect transcript B^t, indicating that it extends into the *HMS2* sense promoter. However, probe H4 at the 3' end of the *HMS2* gene was unable to hybridise to B^t, indicating that B^t initiates upstream of this site. So whilst CRISPRi successfully blocked the original *SUT650*, a new Xrn1-sensitive unstable antisense transcript (B^t) was created. This is potentially due to changes in the chromatin structure caused by AS+148NT/dCas9 binding to this region (Horlbeck, Witkowsky, et al., 2016; Isaac et al., 2016), creating an environment that is permissive for transcription initiation (Murray et al., 2012). We note that using probe H4 we were also unable to detect *SUT650* initiating from its WT start site but terminating at the AS+148NT binding site, due to its small size (~148 nt).

CRISPRi-induced *GAL1* AS repression does not affect the *GAL1* sense transcript

We tested whether *GAL1* AS repression by AS+112NT/dCas9 affected the *GAL1* sense transcript. Previously we mutated a TATA-like sequence to ablate antisense transcription but observed no difference in *GAL1* sense transcript levels in the population (Murray et al., 2015). Using CRISPRi, we also observed no significant change in *GAL1* sense transcript levels or size (Fig. 3A,B). To support a

strand-specific transcriptional block of AS transcription, *GAL1* sense transcript polyA site usage was unaffected by sgRNA AS+112NT/dCas9 (Fig. 3C). Furthermore, *XRN1* deletion in this strain also did not affect polyA site usage, ruling out a partial double-stranded transcriptional block and subsequent destabilisation of the resulting truncated sense transcript (Fig. 3C).

CRISPRi-induced *SUT650* repression truncates the *HMS2* sense transcript

Previous work shows that reducing *SUT650* transcription increases *HMS2* sense transcript levels (Nguyen et al., 2014). However, blocking *SUT650* by AS+148NT/dCas9 did not similarly increase *HMS2* sense levels (Fig. 3D, lanes 1&3). To our surprise, in addition to the full-length *HMS2* sense transcript (A), we detected a considerably shortened *HMS2* sense transcript (A^t). Since the combined levels of the truncated and full-length transcripts are similar to those in the strain not expressing an sgRNA, independent of the presence of *XRN1* (Fig. 3D, lanes 1&3 or 2&6), we hypothesised that the AS+148NT/dCas9 complex bound within the *HMS2* coding region may be causing partial premature sense transcription termination, leading to transcript A^t. Thus, we mapped the 3' end of *HMS2* S by Northern blotting using a series of strand-specific probes across the locus (Fig. 3E). Both transcripts A and A^t could clearly be detected using the probes upstream of the AS+148NT/dCas9 binding site (probes H1, H2, H3) but the truncated transcript was undetectable using probe H4 downstream of this site. Thus the transcriptional block caused by AS+148NT/dCas9 is not strand-specific and re-defines the transcriptional landscape at the *HMS2* locus by creating a chromatin environment that is suitable for both transcription initiation and termination. As an additional control, we designed three sgRNAs to block the *HMS2* sense transcripts (S+77NT, S+106NT, S+179NT) and monitored their effects on both *HMS2* sense and antisense transcripts (Fig. 3 – Figure Supplement 1). However, we observed no effect on either levels or integrity.

CRISPRi-induced antisense repression at *HMS2* and *GAL1* is not as efficient as previous methods

We compared the repression efficiency of CRISPRi with our previously used genetic interventions. At *GAL1,* mutation of a TATA-like sequence within the *ADH1* terminator greatly reduced the level of the

GAL1 antisense transcript (Fig. 4A,B) (Murray et al 2015). *XRN1* deletion in this strain only slightly increased *GAL1* AS levels, suggesting that most repression was at the level of transcription rather than altering transcript stability (Fig. 4B,C). By contrast, *XRN1* deletion in the strain expressing AS+112NT/dCas9 did result in some upregulation of *GAL1* AS (Fig. 4B,C), indicating that antisense transcript repression was not as great in this strain. Unlike at *HMS2* (Fig. 2F,G), this stabilised *GAL1* AS transcript was the same size as in the control and so likely represents stabilisation of the transcripts escaping repression rather than novel transcripts.

Next we compared the efficacy of AS+148NT/dCas9 with previous experiments to ablate *SUT650*, where we replaced the entire *HMS2* coding region, including the antisense TSS with the *URA3* coding region (*HMS2:URA3*) (Nguyen et al., 2014). This successful block of *SUT650* transcription increased levels of the *HMS2* sense transcript, the di-cistronic *HMS2-BAT2* transcript and consequently decreased levels of the downstream gene, *BAT2*, due to transcriptional interference (Fig. 4D-F). Whilst CRISPRi resulted in a similar decrease in *SUT650* as *HMS2:URA3*, neither the *HMS2*, *BAT2* nor *HMS2-BAT2* di-cistronic transcripts were altered (Fig. 4F). The discovery that whilst AS+148NT/dCas9 represses *SUT650*, a new unstable *HMS2* antisense transcript is induced and the sense transcript is prematurely terminated could explain why blocking *SUT650* using CRISPRi and the *URA3* gene body replacement strategies did not give the same results (Fig. 4F). Thus CRISPRi is not as effective as a genetic mutation in reducing levels of either the *GAL1* or *HMS2* AS transcripts.

Concluding remarks

Although CRISPRi has been used to strand-specifically repress antisense transcription at *GAL10* (Lenstra et al., 2015) and *GAL1* (this work), here we demonstrate that this is not true at *HMS2*. This may reflect the vastly different transcription levels for the galactose inducible genes (high) compared to *HMS2* (low). Furthermore, a study in human K562 cells found that CRISPRi-induced repression did not correlate with which strand was targeted at 49 genes, although the mechanism behind this observation was not investigated (Gilbert et al., 2014).

175 This work extends our previous hypothesis (Nguyen et al., 2014), allowing us to propose that, rather
176 than acting as a roadblock, the binding of the sgRNA/dCas9 complex at *HMS2* creates a new
177 chromatin environment, which is permissible for transcription initiation and termination. Thus, new
178 transcription units are generated that result in novel sense and antisense transcripts of varying
179 stabilities that are therefore not always detectable. This redefinition of the transcriptional landscape
180 highlights the levels of controls and locus understanding needed before results from using CRISPRi
181 can be interpreted.

182 **AUTHOR CONTRIBUTIONS**

183 Conception and design: FSH, AE-S, TB, JM; Acquisition of data: FSH, AR, AN; Analysis and
184 interpretation of the data: FSH, AR, AN, JM; Drafting or revising the manuscript: FSH, TB, JM;
185 Contributed unpublished, essential data, or reagents: AE-S.

186 **FUNDING**

187 The work was funded by the BBSRC (BB/J001694/2).

188 **CONFLICT OF INTEREST**

189 J.M holds stock in Oxford BioDynamics Ltd., Chronos Therapeutics Ltd., and Sibelius Ltd. but these
190 holdings present no conflict of interest with work in this article. The other authors have declared no
191 conflicts of interest.

192 **ACKNOWLEDGEMENTS**

193 The authors thank Jack Feltham for assistance with sgRNA template construction.

194

REFERENCES

Bassett, A. R., Akhtar, A., Barlow, D. P., Bird, A. P., Brockdorff, N., Duboule, D., … Ponting, C. P. (2014). Considerations when investigating lncRNA function in vivo. *eLife*, *3*(August2014), 1–14. http://doi.org/10.7554/eLife.03058

Birts, C. N., Sanzone, A. P., El-Sagheer, A. H., Blaydes, J. P., Brown, T., & Tavassoli, A. (2014). Transcription of click-linked DNA in human cells. *Angewandte Chemie - International Edition*, *53*(9), 2362–2365. http://doi.org/10.1002/anie.201308691

Dicarlo, J. E., Norville, J. E., Mali, P., Rios, X., Aach, J., & Church, G. M. (2013). Genome engineering in Saccharomyces cerevisiae using CRISPR-Cas systems. *Nucleic Acids Research*, *41*(7), 4336–4343. http://doi.org/10.1093/nar/gkt135

El-Sagheer, A. H., & Brown, T. (2010). Click chemistry with DNA. *Chemical Society Reviews*, *39*(4), 1388–1405. http://doi.org/10.1039/b901971p

El-Sagheer, A. H., & Brown, T. (2011). Efficient RNA synthesis by in vitro transcription of a triazole-modified DNA template. *Chemical Communications (Cambridge, England)*, *47*(44), 12057–8. http://doi.org/10.1039/c1cc14316f

El-Sagheer, A. H., Sanzone, A. P., Gao, R., Tavassoli, A., & Brown, T. (2011). Biocompatible artificial DNA linker that is read through by DNA polymerases and is functional in Escherichia coli. *Proceedings of the National Academy of Sciences of the United States of America*, *108*(28), 11338–43. http://doi.org/10.1073/pnas.1101519108

Gilbert, L. A., Horlbeck, M. A., Adamson, B., Villalta, J. E., Chen, Y., Whitehead, E. H., … Weissman, J. S. (2014). Genome-scale CRISPR-mediated control of gene repression and activation. *Cell*, *159*(3), 647–661. http://doi.org/10.1016/j.cell.2014.09.029

Gilbert, L. A., Larson, M. H., Morsut, L., Liu, Z., Brar, G. A., Torres, S. E., … Qi, L. S. (2013). CRISPR-mediated modular RNA-guided regulation of transcription in eukaryotes. *Cell*, *154*(2), 442–451. http://doi.org/10.1016/j.cell.2013.06.044

Horlbeck, M. A., Gilbert, L. A., & Villalta, J. E. (2016). Compact and highly active next-generation libraries for CRISPR-mediated gene repression and activation. *eLife*, *9*, 1–20. http://doi.org/10.7554/eLife.19760

Horlbeck, M. A., Witkowsky, L. B., Guglielmi, B., Replogle, J. M., Gilbert, L. A., Villalta, J. E., … Weissman, J. S. (2016). Nucleosomes impede cas9 access to DNA in vivo and in vitro. *eLife*, *5*(MARCH2016), 1–21. http://doi.org/10.7554/eLife.12677

Isaac, R. S., Jiang, F., Doudna, J. A., Lim, W. A., Narlikar, G. J., & Almeida, R. A. (2016). Nucleosome breathing and remodeling constrain CRISPR-Cas9 function. *eLife*, *5*, e13450. http://doi.org/10.7554/eLife.13450

Knight, B., Kubik, S., Ghosh, B., Bruzzone, M. J., Geertz, M., Martin, V., … Shore, D. (2014). Two distinct promoter architectures centered on dynamic nucleosomes control ribosomal protein gene transcription. *Genes and Development*, *28*(15), 1695–1709. http://doi.org/10.1101/gad.244434.114

Lavender, C. A., Cannady, K. R., Hoffman, J. A., Trotter, K. W., Gilchrist, D. A., Bennett, B. D., … Archer, T. K. (2016). Downstream antisense transcription predicts genomic features that define the specific chromatin environment at mammalian promoters. *PLOS Genetics*, *12*(8), e1006224. http://doi.org/10.1371/journal.pgen.1006224

Lenstra, T. L., Coulon, A., Chow, C. C., & Larson, D. R. (2015). Single-Molecule Imaging Reveals a

238 Switch between Spurious and Functional ncRNA Transcription. *Molecular Cell*, *60*, 1–14.
239 http://doi.org/10.1016/j.molcel.2015.09.028

240 Mali, P., Yang, L., Esvelt, K. M., Aach, J., Guell, M., Dicarlo, J. E., … Church, G. M. (2013). RNA-guided
241 human genome engineering via Cas9. *Science*, *339*(February), 823–827.
242 http://doi.org/10.1126/science.1232033

243 Mellor, J., Woloszczuk, R., & Howe, F. S. (2016). The Interleaved Genome. *Trends in Genetics*, *32*(1),
244 57–71. http://doi.org/10.1016/j.tig.2015.10.006

245 Murray, S. C., Haenni, S., Howe, F. S., Fischl, H., Chocian, K., Nair, A., & Mellor, J. (2015). Sense and
246 antisense transcription are associated with distinct chromatin architectures across genes.
247 *Nucleic Acids Research*, *43*(16), 7823–7837. http://doi.org/10.1093/nar/gkv666

248 Murray, S. C., Serra Barros, A., Brown, D. A., Dudek, P., Ayling, J., & Mellor, J. (2012). A pre-initiation
249 complex at the 3'-end of genes drives antisense transcription independent of divergent sense
250 transcription. *Nucleic Acids Research*, *40*(6), 2432–44. http://doi.org/10.1093/nar/gkr1121

251 Nguyen, T., Fischl, H., Howe, F. S., Woloszczuk, R., Barros, A. S., Xu, Z., … Mellor, J. (2014).
252 Transcription mediated insulation and interference direct gene cluster expression switches.
253 *eLife*, *3*, 1–21. http://doi.org/10.7554/eLife.03635

254 Pelechano, V., & Steinmetz, L. M. (2013). Gene regulation by antisense transcription. *Nature*
255 *Reviews. Genetics*, *14*(12), 880–93. http://doi.org/10.1038/nrg3594

256 Pelechano, V., Wei, W., & Steinmetz, L. M. (2013). Extensive transcriptional heterogeneity revealed
257 by isoform profiling. *Nature*, *497*(7447), 127–31. http://doi.org/10.1038/nature12121

258 Pliatsika, V., & Rigoutsos, I. (2015). "Off-Spotter": very fast and exhaustive enumeration of genomic
259 lookalikes for designing CRISPR/Cas guide RNAs. *Biology Direct*, *10*(1), 4.
260 http://doi.org/10.1186/s13062-015-0035-z

261 Qi, L. S., Larson, M. H., Gilbert, L. A., Doudna, J. A., Weissman, J. S., Arkin, A. P., & Lim, W. A. (2013).
262 Repurposing CRISPR as an RNA-guided platform for sequence-specific control of gene
263 expression. *Cell*, *152*(5), 1173–83. http://doi.org/10.1016/j.cell.2013.02.022

264

MATERIALS AND METHODS

sgRNA design

PAM sequences within 200 bp of the TSS in question were identified and the 20 bp immediately adjacent to these were used to design the variable regions of the sgRNAs. These sequences were run through an off-spotter algorithm (https://cm.jefferson.edu/Off-Spotter//) to minimise any off-target effects (Pliatsika & Rigoutsos, 2015). The sequence for the engineered constant region and *SUP4* terminator were taken from (Dicarlo et al., 2013; Mali et al., 2013). The *HMS2* sgRNA templates were synthesised as two DNA oligonucleotides to be joined by click chemistry, with the majority of the constant region on one oligonucleotide that could be used for all reactions. To increase the efficiency of the click reaction, the click linkage was designed between a dCpT dinucleotide within the Cas9 handle region. The sequences for the *HMS2* and *GAL1* sgRNAs are shown in Supplementary File 1. Full-length sgRNA templates were also synthesised for the *GAL1* sgRNAs and as a control for the *HMS2* click chemistry constructs (Eurofins Genomics).

Click chemistry

Single-stranded DNA oligonucleotides complementary to the constant and variable sgRNA regions were synthesised by standard phosphoramidite oligonucleotide synthesis with 3'-alkyne or 5'-azido modifications respectively (El-Sagheer et al., 2011) (Supplementary File 1). The click chemistry reaction was performed with a Cu^{1} catalyst and 24-30 nt splint DNAs (El-Sagheer et al., 2011). PCR was performed for second strand synthesis, amplification and incorporation of sequences homologous to the site of insertion in *S. cerevisiae*. PCR efficiencies were obtained using qPCR performed three times with four serial 10-fold dilutions in triplicate (Corbett 6000 Rotorgene software).

Strain construction

dCas9, without fusion to a transcriptional repressor domain, was expressed from a plasmid (# 46920 Addgene (Qi et al., 2013)) under the control of the *TDH3* promoter. The DNA templates for sgRNA production were integrated in place of an exogenous *URA3* cassette immediately downstream of the splice site in the endogenous *snR52* locus using homologous recombination followed by 5-FOA selection. Correct insertion was confirmed by genomic DNA sequencing. *SNR52* is a Pol III-transcribed C/D box small nucleolar RNA (snoRNA) gene and so does not undergo extensive post-transcriptional processing such as capping and polyadenylation, and transcripts from this locus are retained in the nucleus. Additionally, the locus contains a self-splicing site that produces a mature

transcript without additional machinery, allowing precise production of a mature sgRNA without any unwanted extensions. Primer sequences for strain construction are listed in Supplementary File 2.

Yeast growth

The strains used in this study are listed in Supplementary File 3. Strains were grown to mid-log at 30°C in complete synthetic media lacking leucine (for dCas9 plasmid selection). For experiments studying the *GAL1* locus, yeast were grown to mid-log in rich media (YP 2% D/YP 2% Gal) so that the *GAL1* induction kinetics were similar to what we had observed previously (Murray et al., 2012, 2015). dCas9 expression was unaffected by the temporary absence of plasmid selection (Fig. 1 – Figure Supplement 1).

Yeast growth controls

Assessment of growth in liquid culture (CSM-leucine) was achieved using a Bioscreen spectrophotometer that automatically measures the optical density of cultures at 30°C every 20 min for 24 h. Doubling times were extracted from the gradient of the curves during logarithmic growth.

Northern blotting

Northern blotting was performed as before (Murray et al., 2012; Nguyen et al., 2014) using asymmetric PCR or *in vitro* transcription with T7 RNA polymerase to generate the radioactive strand-specific probes for *GAL1* and *HMS2* respectively. Primers for these reactions are listed in Supplementary File 4. Northern blots were quantified using ImageJ and images acquired using a Phosphorimager. Images in the figures are scans of exposures to X-ray film.

Western blotting

dCas9 expression was confirmed after each experiment using an anti-Cas9 antibody (Diagenode C15310258) at 1:5000 dilution and anti-Tubulin (Abcam ab6160) at 1:3333.

3’ RACE mapping

Mapping of the 3’ end of the *GAL1* sense transcript was performed as (Nguyen et al., 2014). Primers are listed in Supplementary File 5.

FIGURED AND FIGURE LEGENDS

Figure 1. Experimental strategy for sgRNA template synthesis and incorporation into yeast.

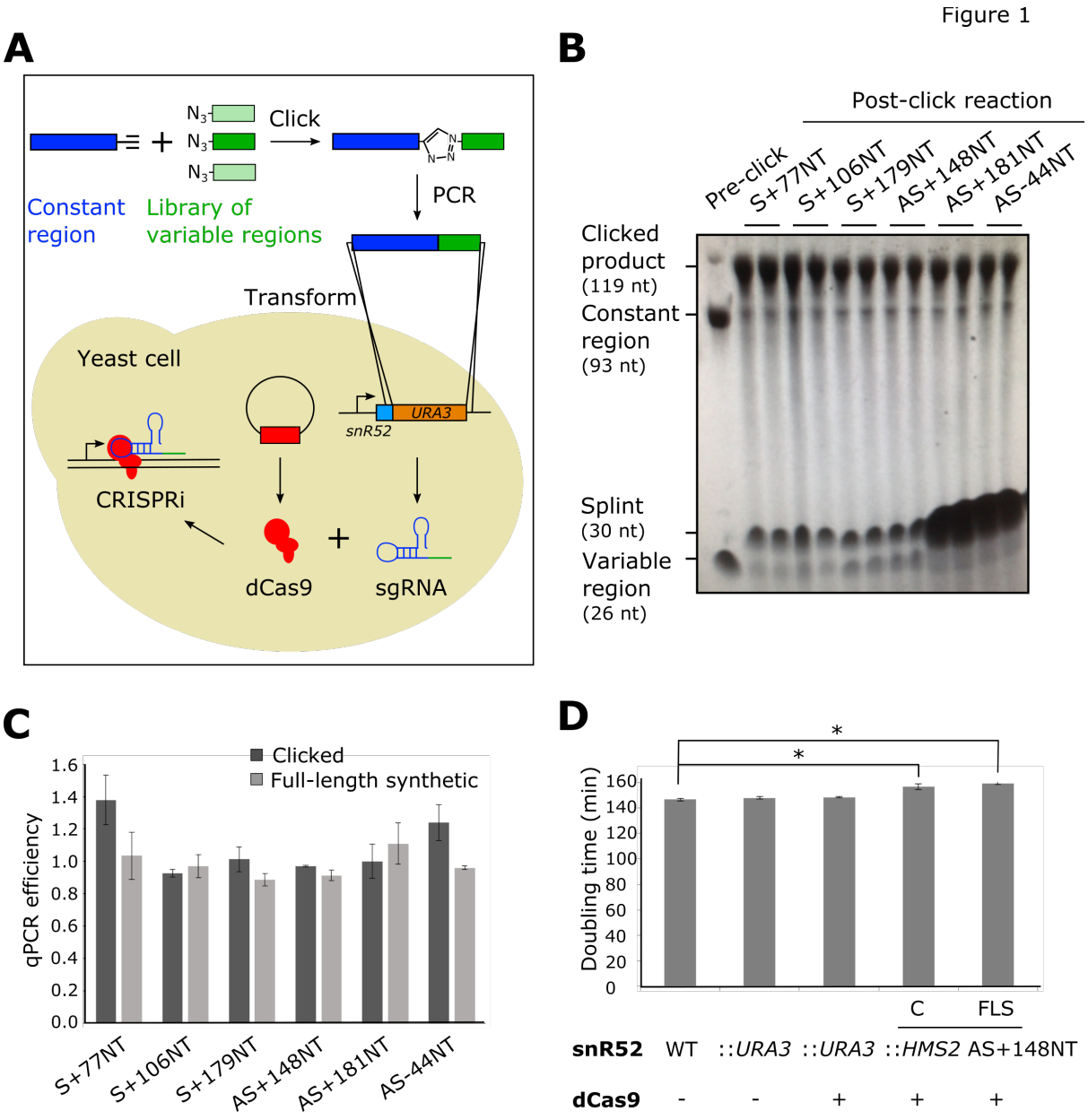

A. An outline of the experiment. Templates for sgRNA production were generated using a click chemistry reaction between a single-stranded DNA oligonucleotide with a 3' alkyne group encoding the constant region (dark blue) and a number of single-stranded DNA oligonucleotides with 5' azido groups encoding the different variable regions (green). The resulting single-stranded DNA oligonucleotide was purified, amplified by PCR and transformed into yeast to replace the *URA3* selection cassette that had previously been introduced into the endogenous *snR52* locus. Correct insertion was confirmed by Sanger sequencing. The expression of the sgRNA is driven from the endogenous RNA polymerase III *snR52* promoter and processed to produce a mature sgRNA. The

sgRNA couples with enzymatically dead Cas9 (dCas9, red) expressed under the control of the *TDH3* promoter off a plasmid to block transcription. See Methods for more detail. **B.** A polyacrylamide gel visualised by UV shadowing reveals a high efficiency of the click reaction for all the *HMS2* constructs (see Figures 2E and Figure 3 – Figure Supplement 1 for positions of the sgRNA binding sites). The sizes of the variable region, DNA splint, constant region and clicked product are indicated. **C.** PCR efficiencies of the clicked and full-length synthetic DNA oligonucleotides as measured by qPCR with a serial dilution series. N=3, errors are standard error of the mean (SEM), all differences are not significant p>0.05. **D.** Doubling times (min) of the indicated yeast strains grown in complete synthetic media minus leucine. C, strains constructed using clicked oligonucleotides; FLS, strains constructed using full-length synthetic oligonucleotides. N=10, errors are SEM, * p<0.05.

Figure 1 - Figure Supplement 1. Levels of dCas9 protein in the experimental strains.

Figure S1:

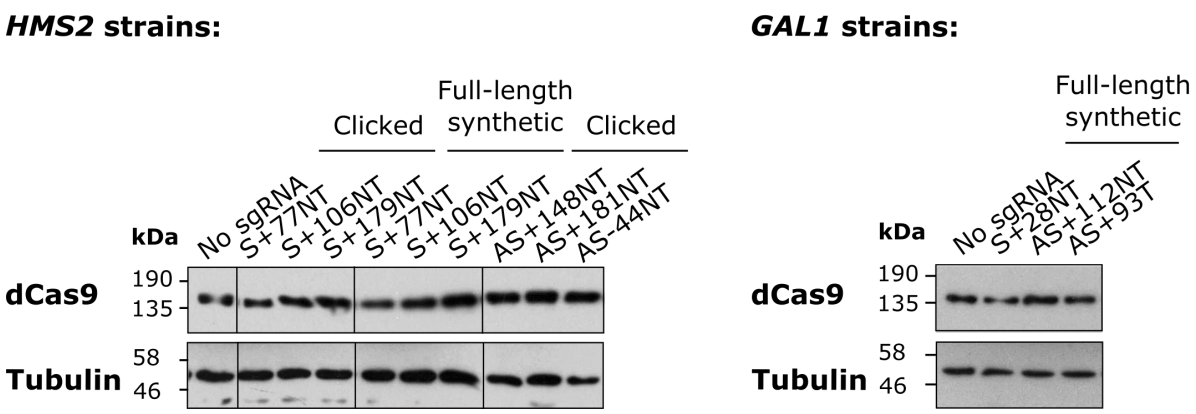

A Western blot showing levels of dCas9 produced in the strains expressing the indicated sgRNAs against *HMS2* (left panel) and *GAL1* (right panel). Tubulin levels are used as a loading control. Images are taken from the same gels with the same exposure times but with some lanes spliced out (indicated with vertical lines).

Figure 2. CRISPRi reduces antisense transcripts at *GAL1* and *HMS2*.

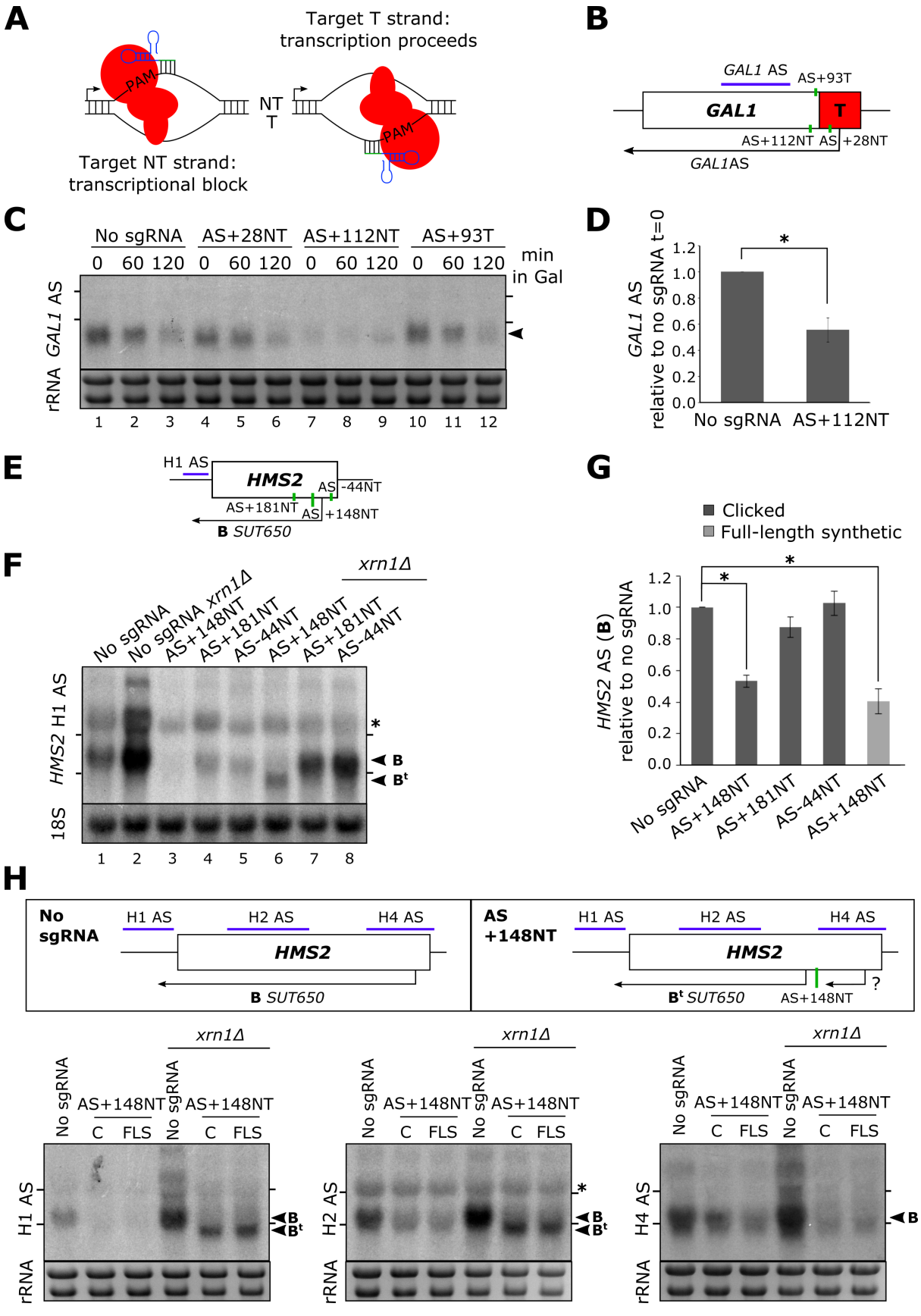

A. A schematic demonstrating the previously reported requirement of non-template strand targeting by the sgRNA/dCas9 complex for strand-specific transcriptional repression. Arrows indicate the direction of transcription. NT, non-template; T, template; red, dCas9; PAM, protospacer adjacent motif; green/blue, sgRNA. **B.** A schematic of the engineered *GAL1* locus showing the site of insertion of the *ADH1* terminator (T, red box), the transcription start site for the stable *GAL1* antisense transcript and the positions of the designed sgRNAs (green vertical lines) targeting the non-template (AS+28NT, AS+112NT) and template (AS+93NT) strands with respect to antisense transcription. The position of the Northern blotting probe detecting the *GAL1* AS transcript is shown in purple. **C.** A Northern blot showing the reduction in *GAL1* antisense transcript (black arrowhead) in the strain expressing sgRNA AS+112NT/dCas9 relative to the no sgRNA control (*GAL1:ADH1*t *snR52::URA3* with dCas9). sgRNAs AS+28NT and AS+93T do not alter *GAL1* AS levels. Samples were taken from cells grown in glucose (t=0) and at the indicated times after transfer to galactose-containing media (min). Positions of the rRNA are indicated by the short horizontal lines. Ethidium bromide-stained rRNA is used as loading control. **D.** Quantification of Northern blotting for the *GAL1* AS transcript at t=0 in the control no sgRNA strain and the strain with sgRNA AS+112NT. N=6, errors are SEM, * $p<0.05$. **E.** A map of the *HMS2* locus showing the *HMS2* AS transcript, *SUT650* (black arrow, transcript B) and positions of the three sgRNAs targeting *SUT650* (green vertical lines). The position of the Northern blotting probe to detect *SUT650* (H1 AS) is shown by the purple line. **F.** A Northern blot probed with *HMS2* antisense probe H1 (see schematic in (**E**)) showing the level of *SUT650* (black arrowhead, transcript B) in the no sgRNA control (*snR52::URA3* with dCas9) strain and strains expressing the indicated antisense-targeting sgRNAs. Deletion of *XRN1* allows detection of a shorter antisense transcript (B^t) in the strain expressing AS+148NT. Positions of the rRNA are indicated by the short horizontal lines. *represents cross-hybridisation with the 26S rRNA. A blot probed for the 18S rRNA is used as loading control. **G.** Quantification of the level of *SUT650* (transcript B) reduction in the strains expressing each of the 3 antisense sgRNAs relative to the control no sgRNA strain. N=4-8, errors represent SEM, *$p<0.05$. Click-linked and full-length synthetic sgRNA AS+148NT templates behave similarly. **H.** Northern blots with a series of *HMS2* antisense-specific probes. A new shorter antisense transcript (B^t) can be detected upon *XRN1* deletion in the strains expressing sgRNA AS+148NT/dCas9. Two clones of the CRISPRi strains produced using clicked (C) or full-length synthetic (FLS) oligos for strain construction are shown. Positions of the antisense-specific probes (purple) and the site of sgRNA AS+148NT/dCas9 binding (green vertical line) are shown in the schematic. Positions of the rRNA on the Northern blot are indicated by the short horizontal lines. *represents cross-hybridisation with the 26S rRNA. Ethidium bromide-stained rRNA is used as loading control.

386 **Figure 2 - Figure Supplement 1. Nucleosome occupancy over the sgRNA target sites does not anti-**
387 **correlate with level of repression.**

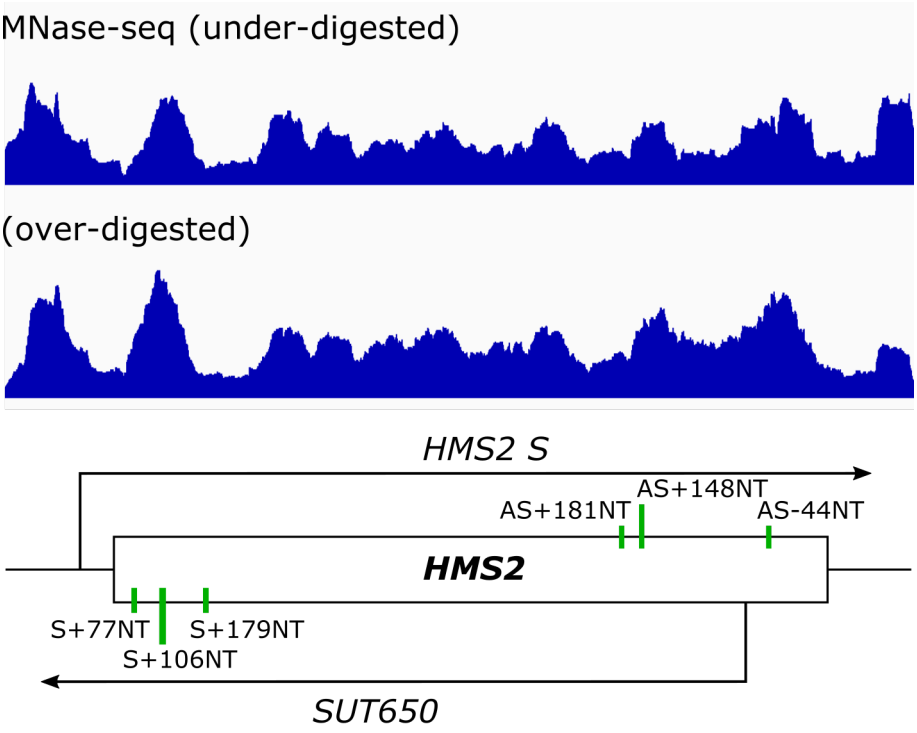

sgRNA	Relative nucleosome occupancy	
	Under	Over
S+77NT	4.295	14.17
S+106NT	16.04	33.99
S+179NT	9.391	11.51
AS+148NT	16.53	19.36
AS+181NT	11.97	15.09
AS-44NT	22.7	28.27

388

389 Nucleosome occupancy map for *HMS2* as measured by sequencing of a sample that has been under-
390 and over-digested with MNase (Knight et al., 2014). The schematic underneath shows the positions
391 of the sgRNA targeting sites. Relative nucleosome occupancy at each sgRNA site is shown in the
392 table for the under- and over-digested samples.

393

394 **Figure 3. *HMS2* and *GAL1* sense transcripts are differently affected by blocking of their respective**

395 **antisense transcripts.**

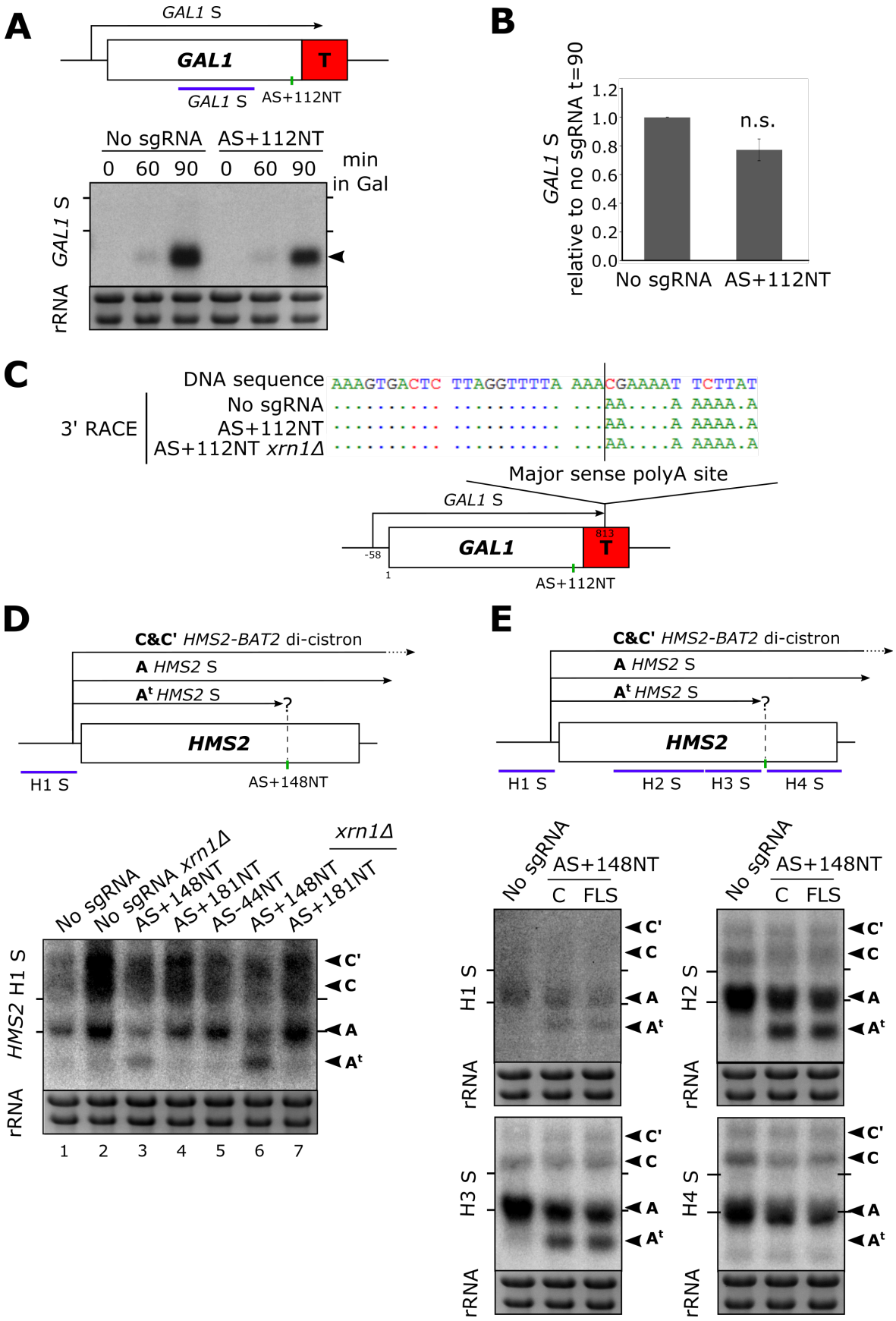

396

A. A Northern blot probed for the *GAL1* sense transcript (black arrow) in the control strain with no sgRNA (*GAL1 ADH1*t *snR52::URA3* with dCas9) and in the strain expressing sgRNA AS+112NT/dCas9. Samples were taken from cells grown in glucose (t=0) and at the indicated times after transfer to galactose-containing media (min). Ethidium bromide-stained rRNA is used as a loading control. **B.** Quantification of the Northern blot shown in (A) at t=90. N=4, error bars represent SEM, change is statistically non-significant (n.s.) p=0.062. **C.** A schematic showing the results of *GAL1* sense transcript 3' end mapping by RACE in the strains indicated. All distances are shown relative to the sense TSS. Transcript cleavage and polyadenylation occurs beyond the position of the *GAL1* AS-blocking AS+112NT sgRNA shown (green vertical line). **D.** A Northern blot probed with *HMS2* sense probe H1 (purple) showing the level of *HMS2* sense (black arrowhead, transcript A) in the no sgRNA control (*snR52::URA3* with dCas9) strain and strains expressing the indicated antisense-targeting sgRNAs. A truncated sense transcript (A^t) was also detected in the strain expressing AS+148NT. Positions of the rRNA are indicated by the short horizontal lines. Ethidium bromide-stained rRNA is used as loading control. **E.** Northern blots with a series of *HMS2* sense-specific probes detecting the regions indicated in the schematic. The position of the sgRNA AS+148NT/dCas9 binding site is shown (green vertical line). Positions of the rRNA are indicated by the short horizontal lines. Ethidium bromide-stained rRNA is used as loading control.

415 **Figure 3 - Figure Supplement 1. *HMS2* sense-targeting sgRNAs/dCas9 do not affect *HMS2* sense or**

416 **antisense transcript levels.**

Figure S3:

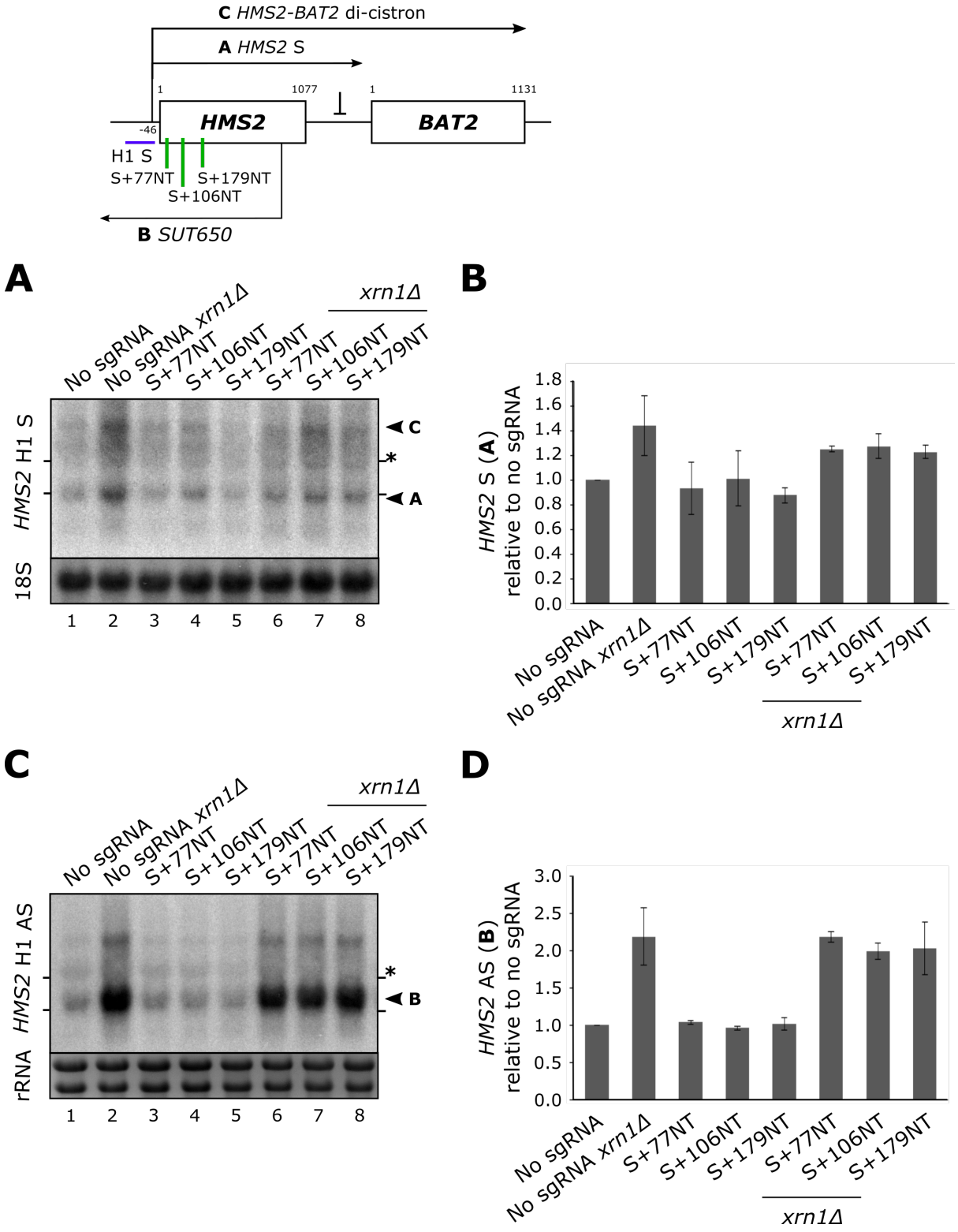

417

418 **A.** A Northern blot probed with *HMS2* sense probe H1 (purple) showing the level of *HMS2* sense

419 (black arrowhead, transcript A) in the no sgRNA control (*snR52::URA3* with dCas9) strain and strains

420 expressing the indicated sense-targeting sgRNAs. Positions of the rRNA are indicated by the short
421 horizontal lines. The 18S rRNA is used as loading control. *represents cross-hybridisation with the
422 26S rRNA. **B.** Quantification of the Northern blot in (A). N=2, errors represent the SEM. **C.** A Northern
423 blot as (A) but probed with *HMS2* antisense-specific probe H1. Ethidium bromide-stained rRNA is
424 used as loading control. **D.** Quantification of the Northern blot in (C). N=2, errors represent the SEM.

425

426 **Figure 4. CRISPRi block of *SUT650* and *GAL1* AS is not as efficient as previous genetic interventions.**

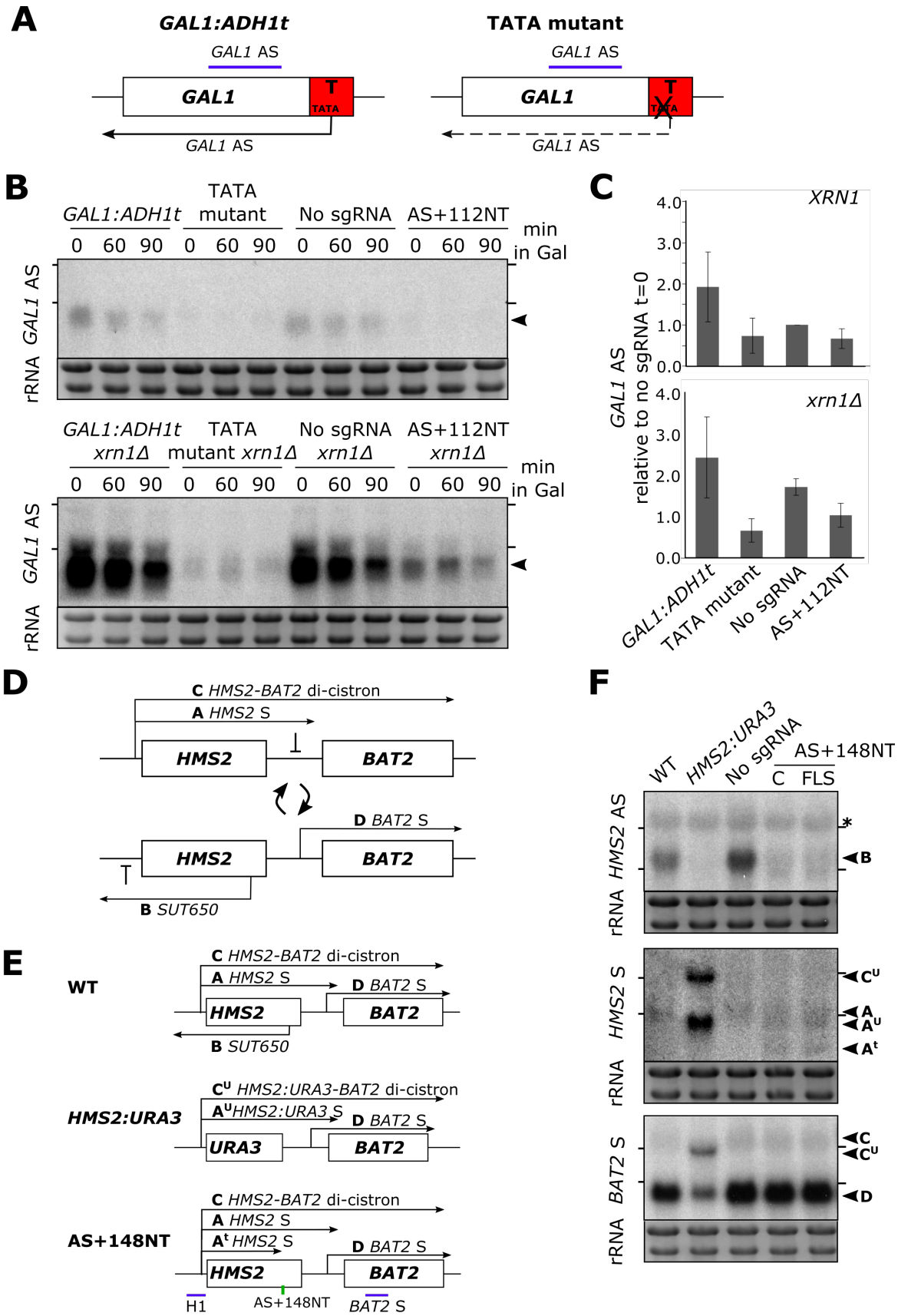

427

A. A schematic showing the previously used genetic intervention to repress the *GAL1* AS transcript (Murray et al., 2015). In the TATA mutant construct, a TATA box within the engineered *ADH1* terminator (T) is scrambled and the level of *GAL1* antisense transcript is reduced. **B.** A Northern blot probed for the *GAL1* antisense transcript (black arrowhead) comparing the two methods of reducing antisense at this locus in the presence (top blot) or absence (bottom blot) of *XRN1*. All samples were run on the same gel and the blots were exposed to film for the same time. Samples were taken from cells grown in glucose (t=0) and at the indicated times after transfer to galactose-containing media (min). Positions of the rRNA are indicated by the short horizontal lines. Ethidium bromide-stained rRNA is used as loading control. **C.** Quantification of the Northern blot in (B) at t=0. N=2, errors represent the SEM. **D.** A schematic of the *HMS2-BAT2* locus, showing the *HMS2* sense and antisense transcripts (A and B), the *HMS2-BAT2* di-cistronic transcripts (C and C') and the *BAT2* sense transcript (D). Cells switch between sense- and antisense-dominant states in which the indicated transcripts are produced (Nguyen et al., 2014). **E.** The *HMS2-BAT2* locus and associated transcripts in the WT strain and strains that repress the *SUT650* transcript. In the *HMS2:URA3* strain, the entire coding region of *HMS2* is replaced by that of *URA3*. **F.** Northern blots comparing the efficiency of *SUT650* reduction by replacement of the *HMS2* coding region with that of *URA3* versus CRISPRi and the relative effects of these two strategies on the *HMS2* sense and *BAT2* transcripts shown in (E). The WT (BY4741) and *HMS2.URA3* strains have been transformed with plasmid pRS315 to allow for growth on complete synthetic media lacking leucine and thus comparisons with the CRISPRi strains. Positions of the rRNA are indicated by the short horizontal lines. *represents cross-hybridisation with the 26S rRNA. Ethidium bromide-stained rRNA is used as loading control.

Supplementary File 1. Templates for sgRNAs

Supplementary File 2. Primers for strain construction

Supplementary File 3. *Saccharomyces cerevisiae* strains used in this study

Supplementary File 4. Primers for construction of Northern blot probe templates

Supplementary File 5. Primers for 3' RACE mapping of the *GAL1* sense transcript

458 **Supplementary File 1. Templates for sgRNAs**

sgRNA template	Sequence 5'-3'
Constant region	AGACATAAAAAACAAAAAAAGCACCACCGACTCGGTGCCACTTTTTCAAGTTGATAACGG ACTAGCCTTATTTTAACTTGCTATTTCTAGCTC
HMS2 S+77NT variable region	TAAAACGATGTCTTTGTAAGCAAACT
HMS2 S+106NT variable region	TAAAACGCTGCAGGGGAACGCTTACT
HMS2 S+179NT variable region	TAAAACGACCAGTTCACCAAAGTCAT
HMS2 AS+148NT variable region	TAAAACCGGGATGCAACTGCGGGTGC
HMS2 AS+181NT variable region	TAAAACTATCCAAAGAGCAGTTCATA
HMS2 AS-44NT variable region	TAAAACACTGCAAAAAATGGTGGAAA
HMS2 S+77NT full-length	AGACATAAAAAACAAAAAAAGCACCACCGACTCGGTGCCACTTTTTCAAGTTGATAACGG ACTAGCCTTATTTTAACTTGCTATTTCTAGCTCTAAAACGATGTCTTTGTAAGCAAACT
HMS2 S+106NT full-length	AGACATAAAAAACAAAAAAAGCACCACCGACTCGGTGCCACTTTTTCAAGTTGATAACGG ACTAGCCTTATTTTAACTTGCTATTTCTAGCTCTAAAACGCTGCAGGGGAACGCTTACT
HMS2 S+179NT full-length	AGACATAAAAAACAAAAAAAGCACCACCGACTCGGTGCCACTTTTTCAAGTTGATAACGG ACTAGCCTTATTTTAACTTGCTATTTCTAGCTCTAAAACGACCAGTTCACCAAAGTCAT
HMS2 AS+148NT full-length	AGACATAAAAAACAAAAAAAGCACCACCGACTCGGTGCCACTTTTTCAAGTTGATAACGG ACTAGCCTTATTTTAACTTGCTATTTCTAGCTCTAAAACCGGGATGCAACTGCGGGTGC
HMS2 AS+181NT full-length	AGACATAAAAAACAAAAAAAGCACCACCGACTCGGTGCCACTTTTTCAAGTTGATAACGG ACTAGCCTTATTTTAACTTGCTATTTCTAGCTCTAAAACTATCCAAAGAGCAGTTCATA
HMS2 AS-44NT full-length	AGACATAAAAAACAAAAAAAGCACCACCGACTCGGTGCCACTTTTTCAAGTTGATAACGG ACTAGCCTTATTTTAACTTGCTATTTCTAGCTCTAAAACACTGCAAAAAATGGTGGAAA
GAL1 AS+28NT full-length	CAAATTTTAAAGTGACTCTTGTTTTAGAGCTAGAAATAGCAAGTTAAAATAAGGCTAGTCC GTTATCAACTTGAAAAAGTGGCACCGAGTCGGTGGTGCTTTTTTTGTTTTTTATGTCT
GAL1 AS+112NT full-length	TGAGTTCAAACCGCAGTTGAGTTTTAGAGCTAGAAATAGCAAGTTAAAATAAGGCTAGTC CGTTATCAACTTGAAAAAGTGGCACCGAGTCGGTGGTGCTTTTTTTGTTTTTTATGTCT
GAL1 AS+93T full-length	TTTTCATGGTTTTTTAATTGGTTTTAGAGCTAGAAATAGCAAGTTAAAATAAGGCTAGTCCG TTATCAACTTGAAAAAGTGGCACCGAGTCGGTGGTGCTTTTTTTGTTTTTTATGTCT

459

460

461 **Supplementary File 2. Primers for strain construction**

Primer	**Sequence 5'-3'**
URA3 insertion into *SNR52* F (template = pRS316)	GATGAATGACATTAGCGTGAACAATCTCTGATACAAAA TCCTGAGAGTGCACCACGCTTT
URA3 insertion into *SNR52* R (template = pRS316)	CAGAAGGAAGGCAACATAAGTTTTTCTAATCCTAAAAT CTGTGCGGTATTTCACACCGCA
sgRNA *HMS2* S+77NT insertion into *SNR52* F	TCGGCGTTCGAAACTTCTCCGCAGTGAAAGATAAATGA TCAGTTTGCTTACAAAGACATC
sgRNA *HMS2* S+106NT insertion into *SNR52* F	TCGGCGTTCGAAACTTCTCCGCAGTGAAAGATAAATGA TCAGTAAGCGTTCCCCTGCAGC
sgRNA *HMS2* S+179NT insertion into *SNR52* F	TCGGCGTTCGAAACTTCTCCGCAGTGAAAGATAAATGA TCATGACTTTGGTGAACTGGTC
sgRNA *HMS2* AS+148NT insertion into *SNR52* F	TCGGCGTTCGAAACTTCTCCGCAGTGAAAGATAAATGA TCGCACCCGCAGTTGCATCCCG
sgRNA *HMS2* AS+181NT insertion into *SNR52* F	TCGGCGTTCGAAACTTCTCCGCAGTGAAAGATAAATGA TCTATGAACTGCTCTTTGGATA
sgRNA *HMS2* AS-44NT insertion into *SNR52* F	TCGGCGTTCGAAACTTCTCCGCAGTGAAAGATAAATGA TCTTTCCACCATTTTTTGCAGT
sgRNA *GAL1* AS+28NT insertion into *SNR52* F	TCGGCGTTCGAAACTTCTCCGCAGTGAAAGATAAATGA TCCAAATTTT AAAGTGACTCTTG
sgRNA *GAL1* AS+112NT insertion into *SNR52* F	TCGGCGTTCGAAACTTCTCCGCAGTGAAAGATAAATGA TCTGAGTTCAAACCGCAGTTGA
sgRNA *GAL1* AS+93T insertion into *SNR52* F	TCGGCGTTCGAAACTTCTCCGCAGTGAAAGATAAATGA TCTTTTCATG GTTTTTTAATTGG
sgRNA insertion into *SNR52* R	AGAGGTGGCATTTTACATAACAATAGTGACAAAAAATA AAAGACATAAAAAACAAAAAAA
SNR52 check F	AGCAAACAGCCACTGACTGT
SNR52 check R	GCGTACTAATGTTTTTTGTT
SNR52 Sequencing F	TTGTAGTGCCCTCTTGGGCTAG

462

463

464 **Supplementary File 3. *Saccharomyces cerevisiae* strains used in this study**

Strain name	Parent	Genotype	Source
BY4741	S288C	MATa; *his3Δ 1; leu2Δ 0; met15Δ 0; ura3Δ*	Euroscarf
snR52::URA3 + dCas9	BY4741	snR52::*URA3* + p*TDH3*-dCas9 (Addgene plasmid 46920, *LEU*)	This study
HMS2 S+77NT	snR52::URA3 +dCas9	snR52::sgRNA *HMS2* S+77NT	This study
HMS2 S+106NT	snR52::URA3 +dCas9	snR52::sgRNA *HMS2* S+106NT	This study
HMS2 S+179NT	snR52::URA3 +dCas9	snR52::sgRNA *HMS2* S+179NT	This study
HMS2 AS+148NT	snR52::URA3 +dCas9	snR52::sgRNA *HMS2* AS+148NT	This study
HMS2 AS+181NT	snR52::URA3 +dCas9	snR52::sgRNA *HMS2* AS+181NT	This study
HMS2 AS-44NT	snR52::URA3 +dCas9	snR52::sgRNA *HMS2* AS-44NT	This study
HMS2 S+77NT *xrn1*	*HMS2* S+77NT	*xrn1*::HISMX6	This study
HMS2 S+106NT *xrn1*	*HMS2* S+106NT	*xrn1*::HISMX6	This study
HMS2 S+179NT *xrn1*	*HMS2* S+179NT	*xrn1*::HISMX6	This study
HMS2 AS+148NT *xrn1*	*HMS2* AS+148NT	*xrn1*::HISMX6	This study
HMS2 AS+181NT *xrn1*	*HMS2* AS+181NT	*xrn1*::HISMX6	This study
HMS2 AS-44NT *xrn1*	*HMS2* AS-44NT	*xrn1*::HISMX6	This study
BY4741 pRS315	BY4741	+pRS315 (*LEU)*	This study
HMS2:URA3	BY4741	*HMS2 Δ(1-1076)::URA3*	(Nguyen et al., 2014)
HMS2:URA3 pRS315	*HMS2:URA3*	+pRS315 (*LEU*)	This study
*GAL1::ADH1*t	BY4741	*GAL1 Δ(758-1587)::ADH1*t	(Murray et al., 2012)
TATA mutant	BY4741	*GAL1 Δ(758-1587)::ADH1*t (scramble TATA #1)	(Murray et al., 2015)
*GAL1::ADH1*t *xrn1*	*GAL1::ADH1*t	*xrn1::KANMX6*	This study
TATA mutant *xrn1*	TATA mutant	*xrn1::HISMX6*	This study
*GAL1::ADH1*t snR52::URA3 +dCas9	*GAL1::ADH1*t	snR52::*URA3* + p*TDH3*-dCas9 (Addgene plasmid 46920, *LEU*)	This study
GAL1 AS+28NT	*GAL1::ADH1*t snR52::URA3	snR52::sgRNA *GAL1* AS+28NT	This study
GAL1 AS+112NT	*GAL1::ADH1*t snR52::URA3 + dCas9	snR52::sgRNA *GAL1* AS+112NT	This study
GAL1 AS+93T	*GAL1::ADH1*t snR52::URA3 +dCas9	snR52::sgRNA *GAL1* AS+93T	This study
GAL1 AS+112NT *xrn1*	*GAL1* AS+112NT	*xrn1::KANMX6*	This study

465

466

467 **Supplementary File 4. Primers for construction of Northern blot probe templates**

Primer	Sequence 5'-3'
HMS2 H1 S F	GACCCGTCCTTCTTTTACCC
HMS2 H1 S T7 R	TAATACGACTCACTATAGGGAGAGACACACTTGGCGACTG
HMS2 H1 AS T7 F	TAATACGACTCACTATAGGGGACCCGTCCTTCTTTTACCC
HMS2 H1 AS R	AGAGACACACTTGGCGACTG
HMS2 H2 S F	GGCGGGCCGCCCGGACTGCG
HMS2 H2 S T7 R	TAATACGACTCACTATAGGGCGGTTTGGTAGGCGTGAAAC
HMS2 H2 AS T7 F	TAATACGACTCACTATAGGGGGCGGGCCGCCCGGACTGCG
HMS2 H2 AS R	CGGGTGCCACTGAGTGGCCG
HMS2 H3 S F	GTTTCA CGCCTACCAA ACCG
HMS2 H3 S T7 R	TAATACGACTCACTATAGGGCGGGTGCCACTGAGTGGCCG
HMS2 H4 S F	TACGACCTTC TTTTCGTCAC
HMS2 H4 S T7 R	TAATACGACTCACTATAGGGCGGGTGCCACTGAGTGGCCG
HMS2 H4 AS T7 F	TAATACGACTCACTATAGGGTACGACCTTC TTTTCGTCAC
HMS2 H4 AS R	GAATGACCCTCAGAGGCAGG
BAT2 S F	AGGCTTACAGAACGGTGGAC
BAT2 S T7 R	TAATACGACTCACTATAGGGGCTCTATCAGGCGTGGAAAC
GAL1 F	TGTGTCGGACTGGTCTAATT
GAL1 R	GATCCATACCGCCATTGTTA
18S F	AGTGAAACTGCGAATGGCTC
18S R	TGCTGGCACCAGACTTGCCC

468

469

470

471 **Supplementary File 5. Primers for 3' RACE mapping of the *GAL1* sense transcript**

Primer	**Sequence 5'-3'**
Adapter Primer (AP)	GCCCACGCGTCGACTAGTACTTTTTTTTTTTTTTT
Universal amplification primer (UAP)	GCCCACGCGTCGACTAGTAC
GAL1 +346 F	TTGATCCTTCTGTGTCGGACTG

472